

Spectral functions of quarks in quark matter

F. Frömel^a, S. Leupold, and U. Mosel

Institut für Theoretische Physik, Universität Giessen, D-35392 Giessen, Germany

Received: 30 September 2002 /

Published online: 22 October 2003 – © Società Italiana di Fisica / Springer-Verlag 2003

Abstract. We present a simple albeit self-consistent approach to the spectral function of light quarks in infinite quark matter. Relations between correlation functions and collision rates are used to calculate the spectral function in an iterative procedure. The quark interactions are described by the $SU(2)$ Nambu–Jona-Lasinio model. Calculations were performed in the chirally restored phase at zero temperature.

PACS. 24.85.+p Quarks, gluons, and QCD in nuclei and nuclear processes – 12.39.Fe Chiral Lagrangians – 12.39.Ki Relativistic quark model

1 Introduction

It is well known that short-range correlations have influence on the properties of nuclear matter and finite nuclei; a substantial amount of high-momentum processes is contained in the nucleon spectral function. There have been many theoretical approaches trying to understand the short-range correlations. Of particular interest are the self-consistent calculations for the spectral function of nucleons in nuclear matter from Lehr *et al.* [1]. The results of their simple model are in good agreement with sophisticated calculations from many-body theory. It is striking that their model is very successful in describing the influence of short-range correlations on the properties of nuclear matter using a simple pointlike nucleon interaction with a constant scattering amplitude.

Motivated by the success of this model we have taken up the concept to investigate the properties of light quarks in infinite quark matter [2]. It is our basic assumption that the properties of the spectral function are dominated by phase space effects and the overall strength of the interaction just like in the case of the nucleons. The detailed structure of the interaction should be relatively unimportant as long as the relative symmetries are respected. We use relations between the spectral function and the collisional self-energies to construct a simple albeit self-consistent model. The spectral function can then be calculated in an iterative process beyond the quasiparticle approximation. The quark interactions are described by the Nambu–Jona-Lasinio (NJL) model [3]. It has the same symmetries as QCD and describes an effective pointlike interaction.

As a first step the model has been applied to the simplest system, namely the chirally restored phase at zero

temperature. Mean-field effects were neglected, diquark condensates that arise in the color superconducting phase were not included. For the collisional self-energies only the lowest-order contributions, the Born diagrams, were considered. In the numerical calculations the influence of the coupling strength and the chemical potential on the properties of the spectral function was investigated.

2 The model

In this section we will briefly review our model. For more details we refer to [2]. The underlying Green's function formalism is discussed in much detail in [4,5]. Note that current quark masses are neglected throughout this work and only systems in thermal equilibrium are considered. We use the Nambu–Jona-Lasinio model to describe the quark interactions in our approach. It is an effective interaction model that was designed to resemble the symmetries of QCD. The $SU(2)$ Lagrangian is given by

$$\mathcal{L}_{\text{NJL}} = \bar{\psi}i\partial\psi + G[(\bar{\psi}\psi)^2 + (\bar{\psi}i\gamma_5\boldsymbol{\tau}\psi)^2], \quad (1)$$

where G is the coupling strength, independent of energy and momentum, and the τ_i are isospin Pauli matrices. Due to the pointlike interaction this model is nonrenormalizable and a three-momentum cutoff Λ is introduced. Currently we do not consider any extensions to the Lagrangian that lead to color superconductivity, cf. [2].

The correlation functions

$$\begin{aligned} ig^>(1, 1') &= \langle \psi(1)\bar{\psi}(1') \rangle, \\ -ig^<(1, 1') &= \langle \bar{\psi}(1')\psi(1) \rangle \end{aligned}$$

are the fundamental elements of our model. In thermal equilibrium they are related to the spectral function \mathcal{A}

^a e-mail: Frank.Froemel@theo.physik.uni-giessen.de

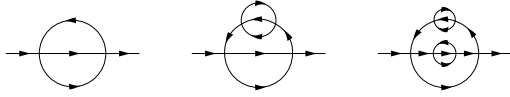


Fig. 1. Examples for diagrams that are resummed in our calculation. The lines correspond to free propagators.

via the thermal Fermi distribution $n_F(p_0)$:

$$-ig^<(p) = \mathcal{A}(p)n_F(p_0), \quad (2)$$

$$ig^>(p) = \mathcal{A}(p)[1 - n_F(p_0)]. \quad (3)$$

Note that the Green's functions and the spectral function are matrices in spinor space. The single-particle self-energy can be decomposed into a mean-field part Σ^{mf} and the collisional self-energies Σ^{\gtrless} . Thus, the retarded self-energy Σ^{ret} is given by

$$\Sigma^{\text{ret}}(1, 1') = \Sigma^{\text{mf}}(1, 1') + \Theta(t_1 - t_{1'}) [\Sigma^>(1, 1') - \Sigma^<(1, 1')]. \quad (4)$$

The time local mean-field self-energy corresponds to the motion of particles in a potential. It is responsible for the dynamical generation of the constituent-quark masses. The collisional self-energies contain the effects of particle decays and collisions in the medium. In lowest order they are given by the Born diagrams (cf. left diagram in fig. 1). One finds

$$\pm i\Sigma^{\gtrless}(p) \sim \iiint \dots G^2 g^{\gtrless}(p_2) g^{\gtrless}(p_3) g^{\gtrless}(p_4), \quad (5)$$

where $g^>$ and $g^<$ are full propagators and the integrals run over p_2, p_3 , and p_4 . Equations (5) look like total collision rates and can be used to determine the width of the spectral function:

$$\Gamma(p) = -2\text{Im}\Sigma^{\text{ret}}(p) = i[\Sigma^>(p) - \Sigma^<(p)]. \quad (6)$$

The real part of Σ^{ret} is related to Γ by a dispersion relation. If the width is known over the full energy range $\text{Re}\Sigma^{\text{ret}}$ can be calculated dispersively. Using Γ and $\text{Re}\Sigma^{\text{ret}}$ the spectral function can be explicitly written as

$$\mathcal{A}(p) = -2\text{Im}g^{\text{ret}}(p) = -2\text{Im} \frac{1}{\not{p} - \text{Re}\Sigma^{\text{ret}} + i\Gamma/2}. \quad (7)$$

Equations (2),(3), and (5)-(7) form a set of equations describing a self-consistency problem. A direct solution is not easily possible. It is possible, however, to solve the problem iteratively by starting from an initial guess for one of the quantities. In this way we can find a solution for the spectral function. The effect of self-consistency can be nicely illustrated in the language of Feynman diagrams. Using full propagators g^{\gtrless} that depend themselves on Σ^{\gtrless} in eqs. (5) means that we sum nonperturbatively over a whole class of diagrams. Some examples are shown in fig. 1.

Finally, we have to discuss the matrix structure of the spectral function in spinor space. To find the most general form \mathcal{A} can be decomposed in terms of the 16 independent products of the γ matrices. Demanding invariance under

parity and time reversal symmetry we find for the rest frame of the medium (in thermal equilibrium) [6]:

$$\mathcal{A}(p) = \rho_s(p_0, \mathbf{p}^2) + \rho_0(p_0, \mathbf{p}^2)\gamma^0 + \rho_v(p_0, \mathbf{p}^2)\hat{\mathbf{p}} \cdot \boldsymbol{\gamma}, \quad (8)$$

where $\hat{\mathbf{p}}$ is a unit vector in the momentum direction. Note that the density of states is given by ρ_0 alone and that ρ_s has to be zero in the chirally restored phase. It follows from eqs. (2)-(7) that Γ and Σ^{\gtrless} must have the same structure as ρ .

Currently we apply two simplifications to the model. First, we restore chiral symmetry ‘‘manually’’ by setting Σ^{mf} to zero. This can be done for any density and temperature since $m = 0$ is always a solution of the equation for the constituent-quark mass [3]. However, one has to be aware that this might not be the thermodynamically favored phase when also a finite solution for m exists. Second, we neglect the real part of Σ^{ret} due to technical reasons [2]. For nuclear matter this was a reasonable approximation [1]. To make sure that the effects of this violation of analyticity are not significant we have checked that $\text{Re}\Sigma^{\text{ret}}$ is small compared to \not{p} , cf. eq.(7).

3 Results

All our calculations were performed at zero temperature and in the chirally restored phase. The calculations were initialized with a constant width, $\Gamma_0 = 1 \text{ MeV}$ and $\Gamma_v = 0$. Self-consistency was achieved after two iterations. First, we chose the quark matter density such that it is comparable to regular nuclear matter, $\rho_{\text{qm}} = 3 \cdot \rho_{\text{nm}} = 3 \cdot 0.17 \text{ fm}^{-3}$. This yields a Fermi energy of $\omega_F = 0.268 \text{ GeV}$. The cutoff Λ and the coupling constant G of the NJL model were chosen so that the model reproduces the known values [3] for the quark condensate and the pion coupling constant f_π in vacuum. To investigate the influence of the coupling on the spectral function we did also calculations with two times and four times larger coupling strengths. In reality quark matter with a chemical potential of $\omega_F = 0.268 \text{ GeV}$ would not be in the chirally restored phase. Therefore we made additional calculations with a higher density of $\rho_{\text{qm}} = 1.53 \text{ fm}^{-3}$, corresponding to $\omega_F = 0.387 \text{ GeV}$. This chemical potential is well beyond the chiral phase transition in the NJL model [3].

Figure 2 shows our results for the spectral function and its width at several momenta and coupling strengths using $\omega_F = 0.268 \text{ GeV}$. Due to the pointlike interaction the width seems to increase explosively for large $|p_0|$. At even higher $|p_0|$, however, the opening of phase space is suppressed by the NJL cutoff and the width decreases again. Physically the most interesting area lies in the energy range $0 < p_0 < \omega_F$ since that is the region of the populated quark states. All states above the Fermi energy as well as the anti-quark states at negative p_0 are unoccupied (no holes in the Dirac sea). The structure of the spectral function is dominated by the on-shell peaks of the quarks and anti-quarks at $p_0 = |\mathbf{p}|$ and $p_0 = -|\mathbf{p}|$. The peaks get broader when the coupling is increased. Strength is distributed away from the peaks to the off-shell regions, the

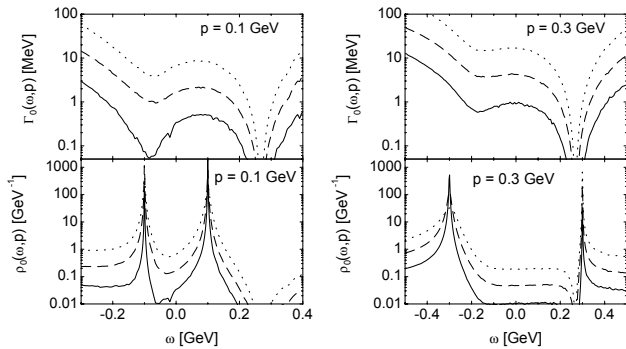


Fig. 2. The width Γ_0 and the spectral function ρ_0 of quarks at different momenta. Solid lines correspond to the usual NJL coupling strength, dashed lines to a coupling twice as large. Dotted lines have been obtained with a coupling four times larger than the usual value.

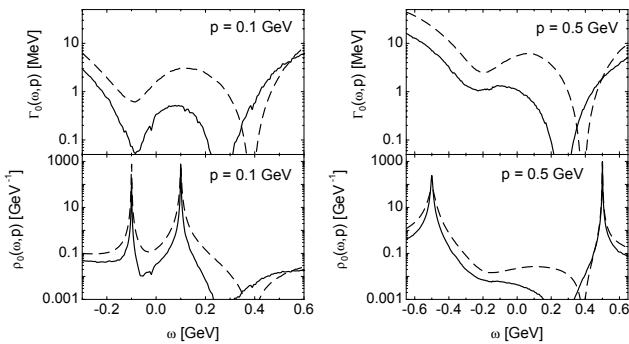


Fig. 3. The width Γ_0 and the spectral function ρ_0 of quarks at different momenta. Solid lines correspond to $\omega_F = 0.268$ GeV, dashed lines to $\omega_F = 0.387$ GeV.

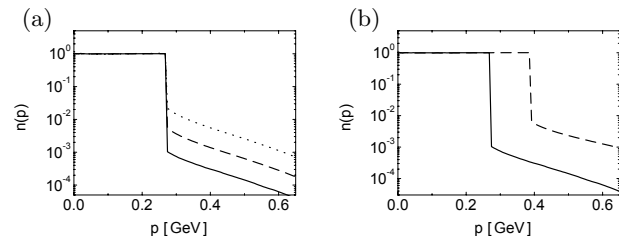


Fig. 4. (a) Quark momentum distribution in quark matter for $\omega_F = 0.268$ GeV and three different couplings (see fig. 2 for details). (b) Momentum distribution for two different chemical potentials (see fig. 3 for details).

width of the peaks increases from 0.1–1 MeV to 10 MeV. The width seems to scale with the coupling strength (respectively G^2 , cf. eqs. (5)) while the general shape remains unchanged.

Figure 3 shows the width and the spectral function for the two chemical potentials $\omega_F = 0.268$ GeV and $\omega_F = 0.387$ GeV using the regular coupling strength. The effect of the higher density is comparable to increasing the coupling. The width approximately scales with the chemical potential while the shape remains unchanged. This leads again to a broadening of the peaks of the spectral function.

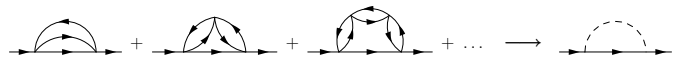


Fig. 5. Series of diagrams corresponding to dynamically generated mesons.

In the momentum distribution of nucleons in nuclear matter a depletion of the occupation probabilities by about 10% is seen [1]. The resulting high-energy tail is taken as a universal sign of short-range correlations. We show the momentum distribution of the quarks for the different coupling strengths in fig. 4(a). At the lowest coupling a depletion of only 0.1% is found. For the coupling twice as large the short-range correlations increase but still the depletion effect is below 1%. Only for the largest couplings we find a high momentum tail of a few percent, comparable to the case of nucleons. In fig. 4(b) it can be seen again that the effect of the larger chemical potential is similar to an increased coupling. The depletion for $\omega_F = 0.387$ GeV grows by almost one order of magnitude compared to $\omega_F = 0.268$ GeV.

4 Summary and outlook

Based on a successful model for nuclear matter we have presented a simple but fully self-consistent approach to the spectral function of quarks in quark matter. It uses a pointlike interaction and goes beyond the quasiparticle approximation. The numerical results indicate that the influence of short-range correlations is rather small compared to nuclear matter. This finding might be an artifact of the present model, the NJL model with vacuum parameters in the Born approximation. Furthermore we have not considered broken symmetries. However, the calculations have shown that the model is technically feasible and suitable for further development.

At present, the model is extended in two ways. First, a more realistic phase with broken symmetries—the chirally broken phase—is considered. In this phase large constituent-quark masses must be taken into account and the analytic structure of the spectral function (8) is more complicated. Second, a new class of diagrams is incorporated into the collisional self-energies (5). This series of diagrams is shown in fig. 5. The lowest-order contribution is again the Born diagram. The full series can be interpreted as a dynamically generated meson that couples to the quarks [3,7]. First estimates show that this extension will increase the effective quark coupling and should lead to significantly higher widths of the spectral function. In addition, it will be possible to investigate the properties of the self-consistently calculated pions and sigmas.

This work was supported by DFG.

References

1. J. Lehr, M. Effenberger, H. Lenske, S. Leupold, U. Mosel, Phys. Lett. B **483**, 324 (2000); J. Lehr, H. Lenske, S. Leupold, U. Mosel, Nucl. Phys. A **703**, 393 (2002).

2. F. Frömel, S. Leupold, U. Mosel, Phys. Rev. C **67**, 015206 (2003), nucl-th/0111004.
3. S.P. Klevansky, Rev. Mod. Phys. **64**, 649 (1992).
4. L.P. Kadanoff, G. Baym, *Quantum Statistical Mechanics* (Benjamin, New York, 1962).
5. P. Danielewicz, Ann. Phys. (N.Y.) **152**, 305 (1984).
6. J.D. Bjorken, S.D. Drell, *Relativistic Quantum Fields* (McGraw-Hill, New York, 1965).
7. P. Rehberg, Phys. Rev. C **57**, 3299 (1998).